International Journal of Research in Education Methodology
Vol.3 No.1, June 2013, ISSN: 2278-7690

PERFORMANCE STUDY AND EXPERIMENTAL CYCLES OF TWO STAGE SOLAR HYBRID ADSORPTION REFRIGERATION SYSTEM

BAIJU.V, MURALEEDHARAN. C
Department of Mechanical Engineering
National Institute of Technology Calicut, Kerala, India. PIN-673601
Department of Mechanical Engineering
National Institute of Technology Calicut, Kerala, India. PIN-673601

ABSTRACT

The performance parameters and experimental cycles of a solar adsorption refrigeration system working with the activated carbon-methanol working pair are presented here. Such a system has been fabricated and tested under the conditions of National Institute of Technology Calicut, Kerala, India. The performance parameters such as specific cooling power (SCP), coefficient of performance (COP), solar heating COP, solar cooling COP, uptake efficiency and exergy efficiency are studied. The dependency between the exergy efficiency and cycle COP with the driving heat source temperature for two thermal compressors is also studied. The optimum heat source temperature for the thermal compressor one is determined as 71.4oC and for the other thermal compressor it is 68.20C. The system has a mean cycle COP of 0.196 during day time and 0.335 for night time. The mean SCP values during day time and night time are 47.83 and 68.2, respectively. Experimental results also demonstrate that the adsorption refrigerator has cooling capacity of 47 to 78 W during day time and 57.6 W to 104.4W during night time. This study also presents the analysis of experimental thermodynamic cycle of solar adsorption refrigeration system. Two cycles have been analysed experimentally, one with clear sky and the other partly cloudy. Use of artificial neural network model is proposed in order to predict the performance of the system. After training, it was found that LM algorithm with 9 neurons is most suitable for modeling solar adsorption refrigeration system. The ANN predictions of performance parameters are in good agreement with the experimental values with R2 values close to one and maximum percentage of error less than 5%. The RMS and covariance values are also found to be within the acceptable limits.with

Key words

Solar; Adsorption; Refrigeration; Activated carbon

1. INTRODUCTION

Environmentally friendly refrigerants with zero ozone depletion potential are to be used in the refrigerators and heat pumps according to Montreal protocol to regulate the production and trade of ozone depleting substances such as CFCs and HCFCs. Use of ozone friendly refrigerants and ability to utilize the renewable energy sources prefer the adsorption systems as an alternative to the conventional refrigeration systems [1, 2].

Saha et al [3] proposed a two stage non-regenerative adsorption chiller design and experimental prototype. The experimental results show that the two stage system can be effectively operated with solar heat at 55oC along with a coolant temperature of 30oC. Douss and Meunier [4] reported experiments on two stage adsorptive heat pump. The cycle consisted of two adsorber zeolite-water system at higher temperature stage and activated carbon-methanol at the low temperature stage. The COP of the system was reported as 1.06, which is higher than the COP of an intermittent cycle. The different refrigeration cycles including a two bed cycle with mass recovery [5], a thermal wave cycle [6,7] and a forced convection cycle [8,9] have been studied by different investigators.

The two major processes in the adsorption refrigeration cycle are the adsorption and desorption processes. Since the refrigeration is intermittent, a system with two beds out of phase is necessary to realise the continuity. But if a renewable source like solar energy is used as power the other measures such as sensible heat storage must be taken in to account. This paper presents the performance investigation of a two stage activated carbon- methanol solar adsorption refrigeration system. The system has been designed and tested for its performance in the Solar Energy Centre of NIT Calicut. The

International Journal of Research in Education Methodology
Vol.3 No.1, June 2013, ISSN: 2278-7690

various performance parameters of the system such as COP, SCP, solar heating COP, solar cooling COP, uptake efficiency and exergy efficiency are also studied.

The low COP and SCP values as compared to the conventional refrigeration systems are the barriers for the commercialization of the adsorption refrigeration systems [10,11].For the improvement of the system a detailed computational and thermodynamic analysis must be carried out. The thermodynamic analyses of adsorption systems are complex because of the complex differential equations involved. To simplify this complex process this paper proposes a new approach, Artificial Neural Network, ANN, for the performance predictions of solar adsorption refrigeration system. The advantage of using ANN as compared to the conventional classical approaches is speed, simplicity and capability to learn from the examples. Recently some works about the use of ANNs in energy systems have been published [12-17].

In this study, the ANN approach is used for investigating the performance of solar adsorption refrigeration system. Utilising the data obtained from the experimental system, an ANN model for the system is developed. With the use of this model, various performance parameters of the system namely the coefficient of performance during day and night time, specific cooling power during day and night time, solar heating coefficient of performance and solar cooling coefficient of performance are predicted and compared with the actual values.

1.2 Two Stage Solar Adsorption Refrigeration System

2. System description and experimental procedure

The single stage solar adsorption refrigeration system with a single adsorbent bed has the limitation that it can only be used in intermittent cycle with desorption in day time and adsorption in night time. To overcome this disadvantage, a two stage adsorption refrigeration system has been developed, fabricated and tested at National Institute of Technology Calicut. The schematic of the system is shown in Fig. 1 and its photographic view is shown in Fig. 2. The solar adsorption refrigeration system has been tested under the meteorological conditions of Calicut (latitude of 11.15o N, longitude of 75.49o E) during March-April 2011.

The system utilises a common evaporator placed inside a refrigerator box, a condenser, an expansion device (capillary tube), parabolic solar concentrator, two adsorbent beds and two water tanks. The parabolic solar concentrator used made of stainless steel has an area 3 m2 .The adsorbent used is activated carbon and the refrigerant, methanol.

The heating of water starts in the morning through the solar concentrator by natural circulation. With the increase in temperature of water in tank 1, the temperature in the adsorbent bed 1 increases. This causes the vapour pressure of the adsorbed refrigerant to reach up to the condensing pressure. When the pressure inside the adsorbent bed 1 is nearly equal to the condensing pressure the valve V1 is opened. The desorbed vapour is liquefied in the condenser. The high pressure liquid refrigerant is expanded through the expansion device to the evaporator pressure. The low pressure refrigerant then enters the evaporator, where the refrigerant takes the latent heat from water to be chilled and convert into vapour refrigerant. The low pressure refrigerant vapour is stored in the accumula

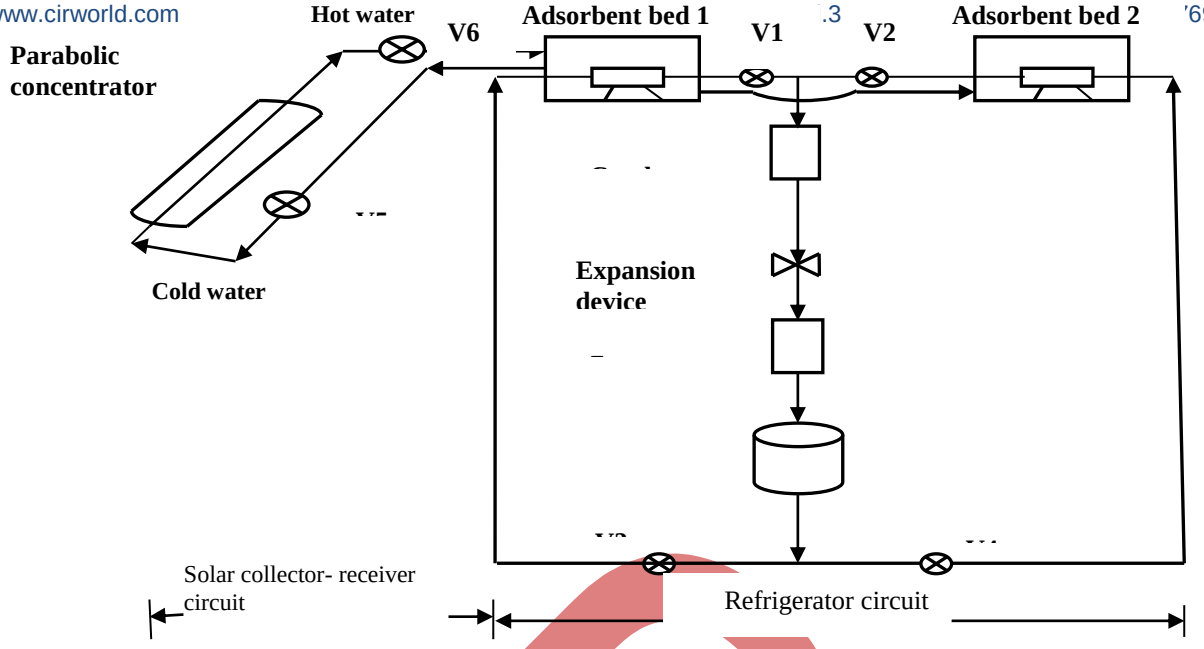

Fig. 1 Schematic diagram of two stage solar adsorption refrigeration system

Fig. 2 Photograph of the experimental set up

During night time bed 1 acts as the adsorber and bed 2 as the desorber. In the evening bed 2 is cooled down by cold water. When the pressure in the bed 2 is nearly equal to the evaporator pressure valve V4 is opened by keeping other valves V1, V2 and V3 closed. After the complete adsorption of refrigerant vapour the hot water from tank 1 is transferred to tank 2, which acts as a heat source for the night time. When the pressure in the bed 2 reaches to the condensing pressure the valve V2 is opened by keeping the valves V1 and V3 closed. The refrigerant passes through the condenser, expansion device and evaporator finally the refrigerant vapour is being stored in the accumulator. During this time the bed 1 acts as adsorber which is cooled down by cooling water to the evaporator pressure so that it is ready for adsorbing the refrigerant stored in the accumulator.

2.2 Adsorbent bed and thermo physical properties of activated carbon used

The adsorbent bed is as shown in Fig. 3. The cross sectional view of the adsorbent bed is as shown in Fig. 4. Both the beds are having the same size and are made of stainless steel. The dimensions of the beds are 400 mm x 400 mm x 180 mm. Activated carbon is selected as adsorbent material and methanol as the refrigerant (activated carbon-methanol

International Journal of Research in Education Methodology
Vol.3 No.1, June 2013, ISSN: 2278-7690

pair) for the system.All the properties of refrigerant used in this paper are taken from REFPROP software. The thermo physical properties of activated carbon used are shown in the Table 1.

Fig. 3 Photograph of adsorbent bed

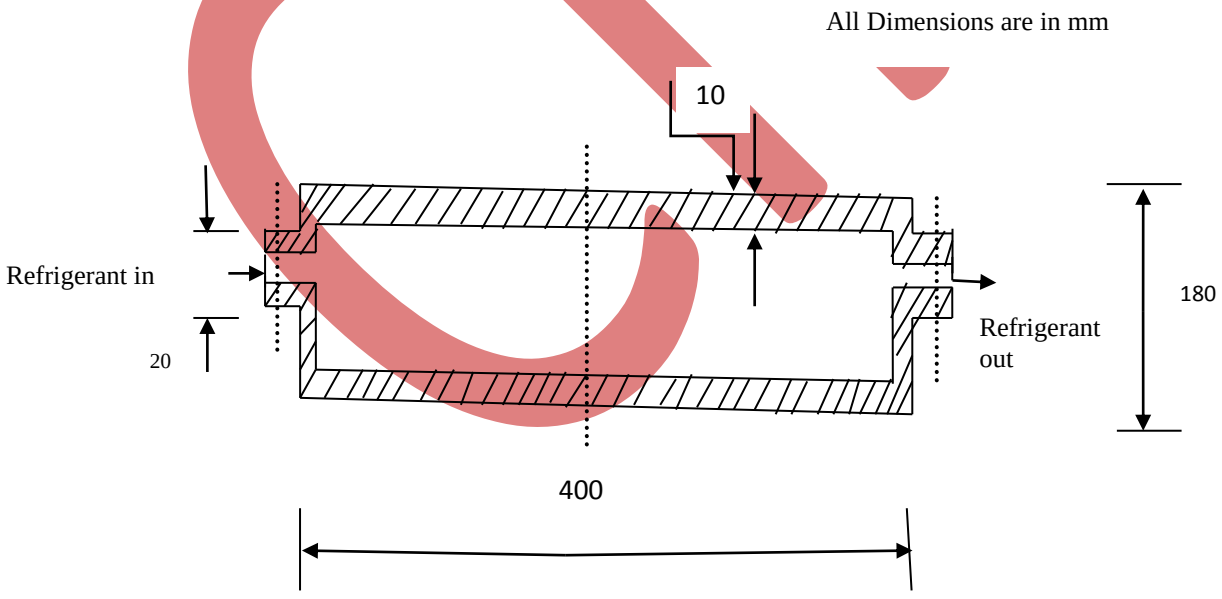

Fig. 4 Cross sectional view of adsorbent bed

International Journal of Research in Education Methodology
Vol.3 No.1, June 2013, ISSN: 2278-7690

Table 1

The thermo physical properties of activated carbon

Type	Granular
Grade	4×8
Particle size	0.25 mm
Surface area	1800 m2g-1
The effective thermal conductivity	0.2 W m-1 K-1
Specific heat	958 J kg-1 K-1
Porosity (%)	50
Effective packing density,ρ_{eff}	115 kg m-3
Solid density ρ_s	525 kg m-3

The thermo physical properties of methanol used

Boiling point	65 0C
Molecular weight	32.04
Purity	99%
Melting point	-980C
The maximum limits of impurities:	
Non volatile substances	0.005%
Aldehydes and ketones ((CH3)2CO)	0.1%
Water	0.2%

Uncertainty analysis

Errors and uncertainties in the experiments can arise from the selection, condition and calibration of the instruments, environment, observation and test planning. A precise method of estimating uncertainty has been presented by Holman [18]. The method is based on a careful specification of uncertainties in the various primary experimental measurements. These measurements are then used to determine some desired results of the experiments. In the present study pressure, temperature and solar insolation are measured by using the instruments. The total uncertainty of the various calculated parameters is shown in Table 2.

Table 2 Uncertainty in different parameters

Description	Total uncertainty (%)
COP daytime	±6.04
COP night time	±5.7
SCP day time	±3.84
SCP night time	±1.89
Heat input to the system	± 1.09
Solar heating COP	±7.5
Solar cooling COP	±2.42

International Journal of Research in Education Methodology
Vol.3 No.1, June 2013, ISSN: 2278-7690

Exergy efficiency	±5.45

Performance parameters

The two most important parameters used for the performance measurement of adsorption refrigeration systems are cycle COP and specific cooling power [19]

Cycle COP

Cycle COP is defined as the ratio of cooling effect to the total energy required for desired cooling effect.

$$\text{COP} = \frac{\text{cooling effect}}{\text{total energy input}}$$

$$\text{COP} = \frac{Q_e}{Q_i} \quad (1)$$

Specific cooling power (SCP)

Specific cooling power indicates the size of the system as it measures the cooling output per unit mass of adsorbent per unit time. Higher SCP values indicate the compactness of the system.

$$SCP = \frac{\text{Cooling effect}}{\text{Cycle time per unit of adsorbent weight}}$$

$$\text{SCP} = \frac{Q_e}{m_{a \times \tau_{cycle}}} \quad (2)$$

4.3 Solar COP

Since the system is solar powered the solar coefficient of performance is also to be defined. This is defined as the ratio of cooling effect to the net solar energy input.

$$\text{Solar COP} = \frac{Q_e}{Q_s} \quad (3)$$

4.4 Uptake efficiency

The thermal uptake efficiency is analogous to the volumetric efficiency of mechanical reciprocating compressor defined as [20].

$$\eta = 1 + \left(\frac{\rho_b - \rho_d}{C_b - C_d}\right)\left(\frac{1}{\rho_{eff}} - \frac{1}{\rho_s}\right) \quad (4)$$

Where $\Delta\rho = \rho_b - \rho_d$ is the difference in the density of the adsorbate between the state points b and d (Fig.5) which is invariably negative since the specific volume decreases due to compression ($\rho_{b<}\rho_d$) consequently the uptake efficiency will be always less than 1. $\Delta\rho$ is determined by the thermodynamic properties of the refrigerant from the knowledge of adsorption and desorption pressure and temperature . ΔC is the combined property of the adsorbent- adsorbate.

ρ_{eff} is the effective packing density of the adsorbent, and ρ_s is the solid density. The effective packing density can be defined as the ratio of the mass of adsorbent that can be packed to the volume of the adsorbent bed.

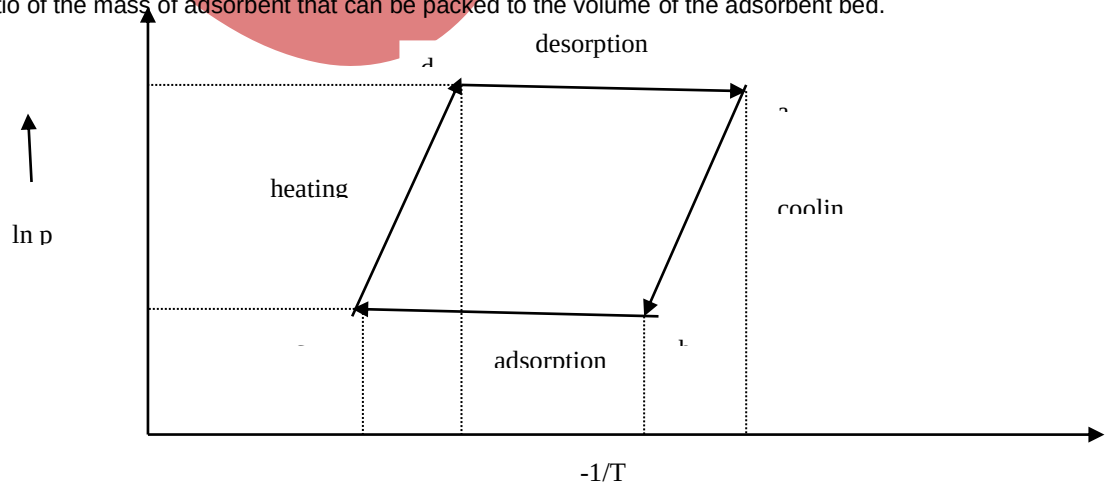

Fig. 5 Clapeyron diagram

International Journal of Research in Education Methodology
Vol.3 No.1, June 2013, ISSN: 2278-7690

Exergy efficiency

$$\text{Exergetic efficiency} = \frac{E_{evap}}{Q_i\left[1-\frac{T_{ref}}{T_{des}}\right]} \quad (5)$$

$$E_{evap} = m\left[(h_1 - h_4) - T_{ref}(s_1 - s_4)\right] \quad (6)$$

ANN modeling of solar adsorption refrigeration system

ANNs are collection of small individual interconnected processing units. The information is passed between these interconnections. They learn the relationship between the input and output. The network usually consists of an input layer, output layer and a hidden layer [13]. ANNs are trained with the known data and tested with the data not used in training. Although the training takes long time they take decision quickly during operation. The performance of ANN based prediction is evaluated by the regression analysis between the network outputs and experimental values. The criteria used for the measurement of network performance are correlation coefficient (R2), root mean square error (RMS) and coefficient of variance (COV) [14].

$$RMS = \left(\frac{1}{n}\sum_{j=1}^{n}\left[t_j - o_j\right]^2\right)^{\frac{1}{2}} \quad (7)$$

$$R^2 = 1 - \left(\frac{\sum_j\left[t_j - o_j\right]^2}{\sum_j (o_j)^2}\right) \quad (8)$$

$$COV = \frac{RMS}{\sum_j o_j} * 100 \quad (9)$$

Where t is the target value, o is the output value, n is the pattern.

The architecture of artificial neural network used for the performance prediction of the system is shown in Fig. 6. In this study the solar insolation, pressure and temperature are given in the input layer where as the coefficient of performance, specific cooling power during night and day time, solar heating coefficient of performance and solar cooling coefficient of performance are obtained in the output layer.

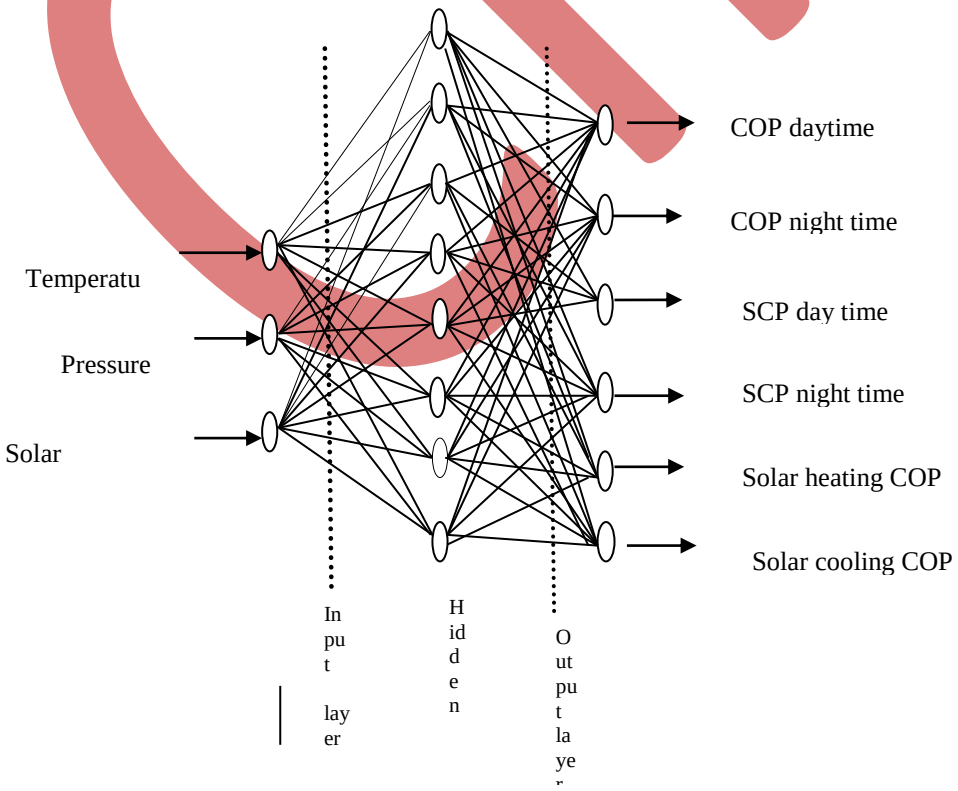

International Journal of Research in Education Methodology
Vol.3 No.1, June 2013, ISSN: 2278-7690

Fig. 6 Neural network for the performance layer prediction of solar adsorption refrigeration system

The feed forward back propagation algorithm with one hidden layer is selected for the study. The variants used in the study are Scaled conjugate gradient (SCG) and Levenberg- Marquardt (LM). The neurons in the input layer have no transfer function. The inputs and outputs are normalized in the range 0-1. Logistic sigmoid (log-sig) transfer function is being used in ANN.

The transfer function used is given by,

$$f(Z) = \frac{1}{1+e^{-Z}} \quad (10)$$

Where Z is the weighted sum of inputs.

The important factor which affects the performance of the ANN is number of neurons in the hidden layer. The system is trained by changing number of neurons from 5 to 10. During each step the performance of the network is studied by using different performance parameters such as R2, RMS and covariance values. During each step the performance of the network is tested and it is decided that the network consists of single hidden layer with 9 neurons and L-M variant is the optimum network for the particular system. The performance parameters of the network with log-sig transfer function and different variants are shown in Table 3. The neural Network tool box in the MATLAB (Version 7.8) is used for the ANN modeling of SAR system

Table 3
Statistical values of different algorithms with different number of neurons

Algorithm	R2	RMS	COV
LM-8	0.9964	0.00161	0.01251
LM-9	0.99981	0.00115	0.01174
LM-10	0.99975	0.00148	0.01961
SCG-8	0.9874	0.00176	0.01276
SCG-9	0.9692	0.00178	0.01905
SCG-10	0.9894	0.00189	0.0104.

The available data obtained from the experimental observations were divided into training and testing sets. The data set consists of 90 input values. From these 80 data sets are used for training and the remaining is used for the testing of network.

Results and discussion

6.1 Experimental observations

The average values of the performance parameters of solar adsorption refrigeration system are shown in Table 4.

Table 4
The average values of performance parameters obtained

Parameters	Value	
Solar cooling COP	0.0758	
Solar heating COP	0.183	
	Day time	Night tim
Refrigerating effect (W)	60.75	79.8
Cycle COP	0.196	0.335
SCP (W/s-kg)	47.83	68.2

6.2 Experimental cycle

The experiments are conducted during the period March-April 2011. The Table 5 shows the adsorbent temperature (T), pressure (P) and concentration (C) for all the cycles limit points obtained. The experimental cycle obtained represents a predominant condition in relation to the cloud cover degree, cycle 1 for clear sky and cycle 2 for partly cloudy.

The thermodynamic cycles obtained are represented in a Concentration-Pressure-Temperature diagram as shown in Figs. 7 and 8. A great deal of information about adsorption and desorption processes can be obtained through the analysis of cycles.

International Journal of Research in Education Methodology
Vol.3 No.1, June 2013, ISSN: 2278-7690

Table 5 The thermodynamic states of experimental cycle 1.

The average Solar Insolation 875 W/m2 (Clear sky) (March 12)

State points	Time	Temperature (oC)	Pressure (bar)	concentration
Regeneration start	9 AM	32.3	0.33	0.42
Desorption start	12.05 PM	64.8	0.682	0.38
Desorption end	3.15 PM	84.4	0.582	0.25
Adsorption start	7.50 PM	38	0.328	0.27
End of adsorption	9.40 PM	27	0.32	0.398

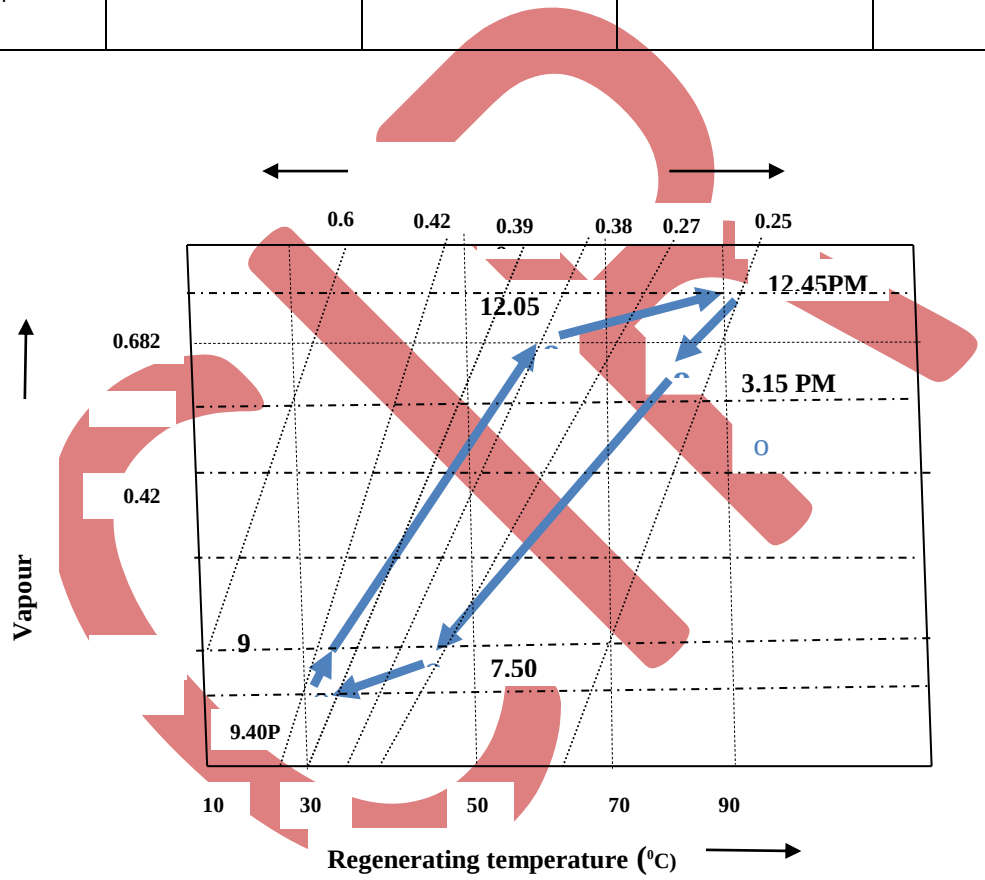

Fig.7 Experimental cycle 1 (March 12, Clear sky)

Table 6 The thermodynamic states of experimental cycle 2.

The Average solar insolation 680 W/m2 (partly cloudy) (April 24)

points	Time	Temperature (oC)	Pressure(bar)	concentration
Regeneration start	9 AM	27.5	0.30	0.44
Desorption start	12.40 PM	64.8	0.682	0.378
Desorption end	2.45 PM	84	0.59	0.302
Adsorption start	7.50 PM	38	0.284	0.335
End of adsorption	8.35PM	27	0.278	0.387

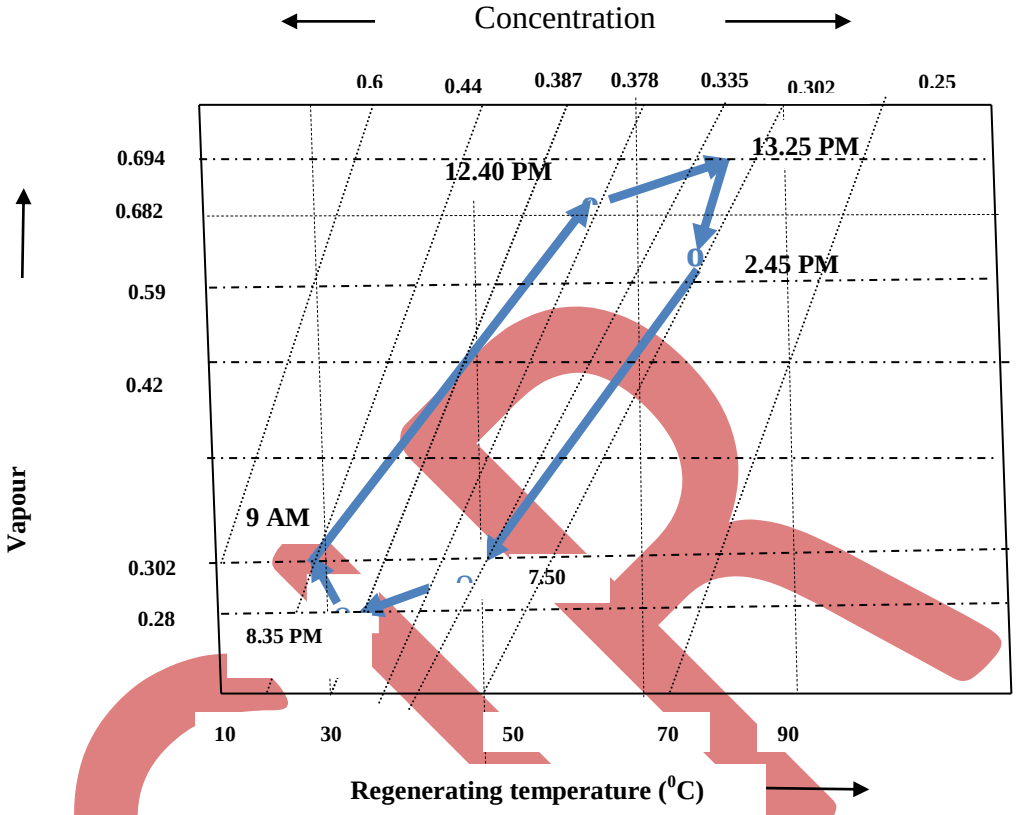

Fig.8 Experimental cycle 2 (April 24, partly cloudy)

The average value of incident solar radiation is 875W/m2 and 680 W/m2 for cycle 1 and cycle 2, respectively. From the Tables 5 and 6 it is clear that the cycle with longest desorption period is for cycle 1. As a result, a larger concentration variation on adsorbate is occurred in this cycle. In this case solar energy is used in much efficient way by the behavior of solar collector components.

From the comparative analysis of these cycles it is noticed that, the cycle with largest adsorption period was cycle 1 (1 h 50 minutes). This can be justified by the greater quantity of previously condensed methanol.

6.2.2 Discrepancies between the ideal and real cycle

The thermodynamic cycles differ from what is theoretically expected mainly in connection with the desorption and adsorption processes which in reality do not happen isobarically as it does in the theoretical cycle shown in Fig. 5.

During the refrigerant transfer to the condenser, adsorbent bed is subjected to a great temperature variation owing to solar radiation incidence, and efficient conversion of this energy into heat. During desorption the adsorbent bed inner temperature is far more influenced by the atmospheric conditions than in the case of adsorption. The adsorption process is more close to an isobar, because the temperature variations in the adsorbent bed during night are smaller, influenced as it is by the ambient air conditions (both temperature and velocity). In relation to the isosteric process small deviations have been noticed both in heating and cooling of adsorbent bed.

6.3 Variation of refrigerant temperature and pressure at typical locations of SAR system

The variations in refrigerant temperature at typical locations in the SAR system working with methanol as refrigerant are as shown in Fig. 9. From the figure it is observed that the average temperature of the refrigerant measured at the thermal compressor suction and exit are 12.4oC and 64.8oC, respectively. The average temperature at the inlet and outlet of expansion device are 42.8oC and 14.2oC, respectively.

The variations in the refrigerant pressure at various points in the refrigeration system are as shown in figure 10. The pressure at thermal compressor inlet and exit varies from 0.18 bar to 0.24 bar and 0.78 bar to 0 .92, respectively. The pressure and temperature at all typical locations of the SAR system get increases with increase in evaporator load.

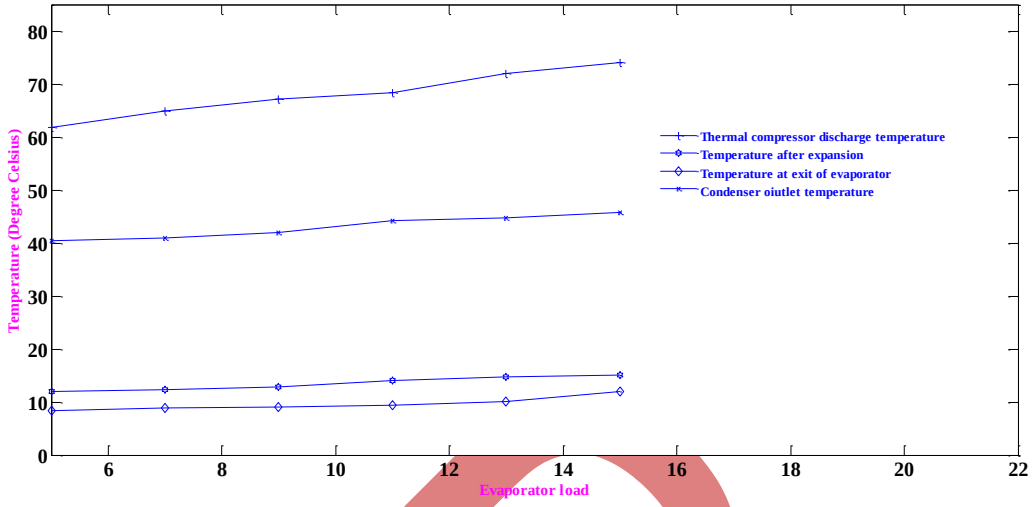

Fig.9 Variations of temperature at typical locations of SAR system

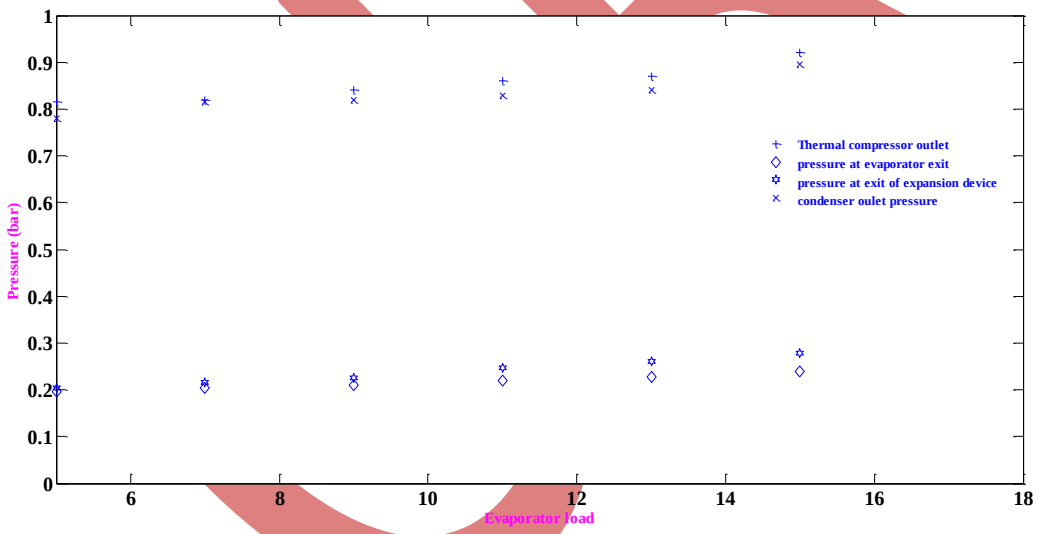

Fig.10 Variations of pressure at typical locations of SAR system

6.3 Pressure transients of thermal compressor

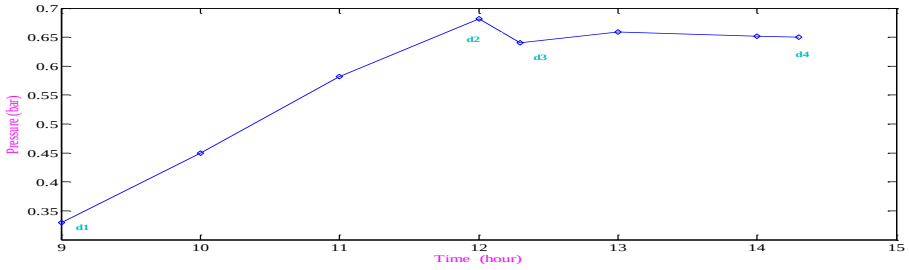

Fig.11 Pressure transients of thermal compressor during heating and desorption phases

International Journal of Research in Education Methodology
Vol.3 No.1, June 2013, ISSN: 2278-7690

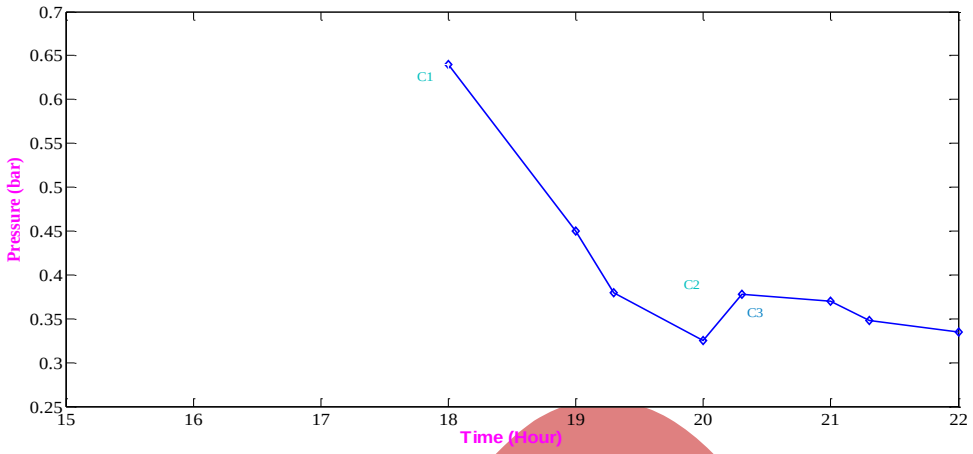

Fig.12 Pressure transients of thermal compressor during cooling and adsorption phases

Figure 11 shows a typical variation of pressure in thermal compressor during the heating and desorption processes. Similarly the Fig. 10 depicts the same for cooling and adsorption phases.

The first order behavior d1-d2 represents typical slow heating of thermal compressor. The dip in pressure seen at d2 is due to the opening of exit valve of thermal compressor. The behavior is exactly same as that in the reciprocating compressor when the discharge reed valve opens. The dip is larger for the larger process time and increases with the increase in desorption temperature.

Figure 12, the first order behavior C1-C2 represents the slow cooling of adsorbent bed. The adsorption of refrigerant begins at 2000 hours and continues up to 2200 hours until full refrigerant is being adsorbed inside the adsorbent bed. The sharp jump seen at C2 is due to the switching from cooling mode to the adsorption phase. The refrigerant is adsorbed inside the adsorbent bed. During this time pressure is increased due to the increase in temperature inside the adsorbent bed due to release of high heat of adsorption.

6.4 Temperature transients in thermal compressor

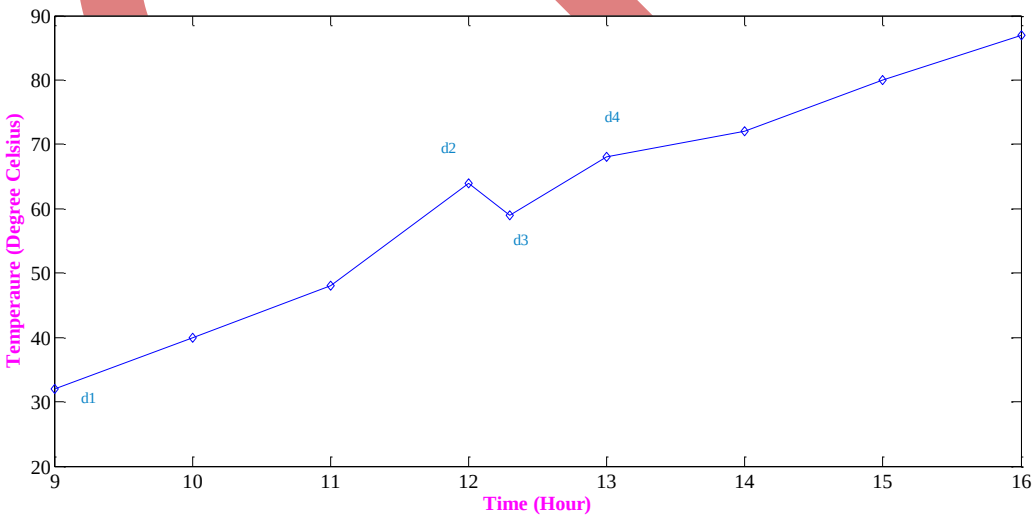

Fig.13 Temperature transients in thermal compressor during heating and desorption phases

International Journal of Research in Education Methodology
Vol.3 No.1, June 2013, ISSN: 2278-7690

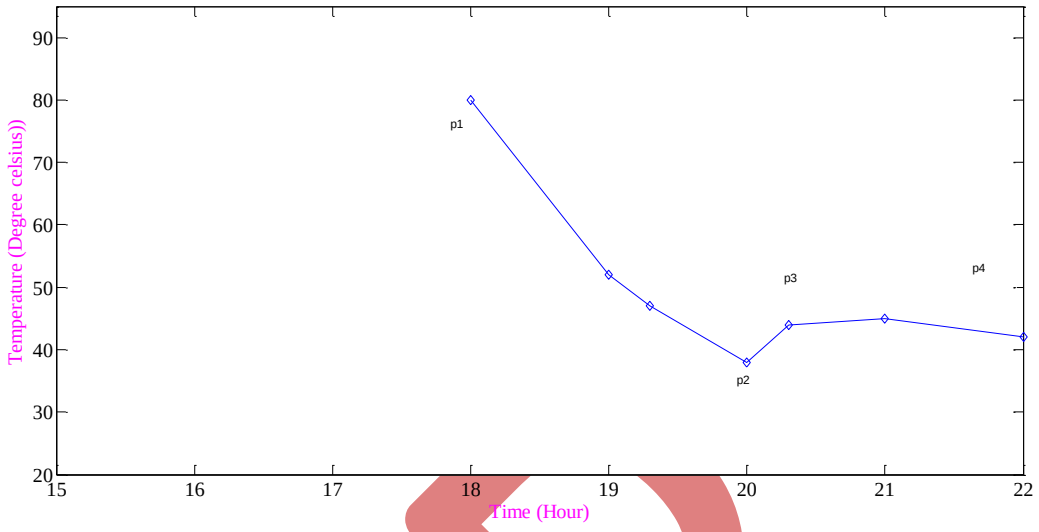

Fig.14 Temperature transients of thermal compressor during adsorption and cooling process

Figure 13 typical variation of the temperature in thermal compressor during the heating and desorption processes. Similarly the Fig.12 depicts the same for cooling and adsorption phases.

The first order behavior d1-d2 represents typical slow heating of thermal compressor. The dip in temperature seen at d2 indicates the start of desorption in thermal compressor. The refrigerant vapour gets desorbed is enters into the condenser.

Figure 14, the first order behavior P1-P2, represents the slow cooling of adsorbent bed. In the evening, the hot water in water tank should be replaced by the cold water so as to make conditions favourable for adsorption. The adsorption of refrigerant begins at2000 hours, and continues up to 2200 hours until full refrigerant is being adsorbed inside the adsorbent bed. There is sharp jump seen at p2 due to the release of high heat of adsorption. From P3-P4 there is a slight increase in the temperature even though the bed is surrounded by the cold water. This is due to the fact that the temperature of surrounding cold water is increased due to the liberation of heat of adsorption. This also leads more adsorption time than it is expected. For overcoming this limitation the water tank with continuous cold water supply is suggested.

6.5 Uptake efficiency

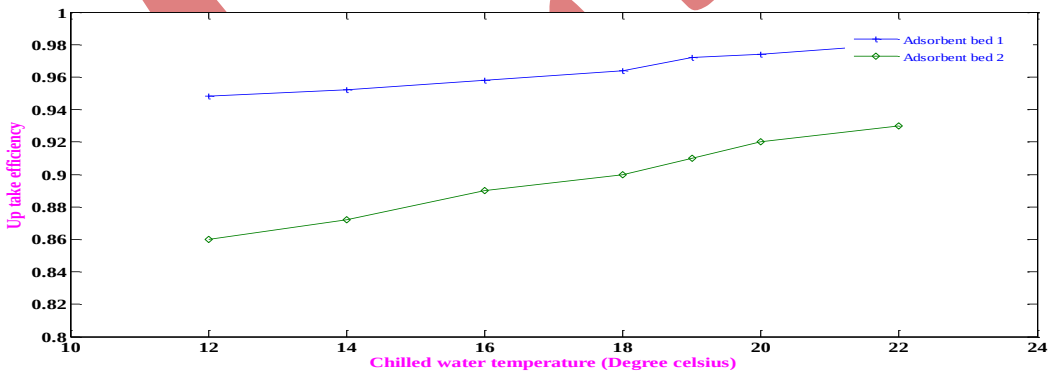

Fig.15 Uptake efficiency variation with evaporator loads

Figure 15 shows the variation of uptake efficiency with evaporator loads for thermal compressor (adsorbent bed) 1 and thermal compressor 2. The uptake efficiency is calculated for activated carbon (particle diameter 0.25 mm) with packing density of 115 kg/m3. For both thermal compressors the uptake efficiency is nearly equal to 1. The uptake efficiency increases with increase in evaporator loads, this augmentation is because of a large concentration difference available at higher evaporator loads. From the figure it is clear that the uptake efficiency is more for the thermal compressor 1 than for the thermal compressor 2. This is because of the adsorption taking place in the thermal compressor 2 during day time, while in the thermal compressor 1 adsorption takes place during night time.

During day time the thermal compressor 2 is subjected to a great temperature variation owing to solar radiation incidence, and efficient conversion of this energy into heat. During adsorption in the thermal compressor 2 the inner temperature is far more influenced by the atmospheric conditions than in the case of thermal compressor (adsorbent bed) 1. The temperature variations in the thermal compressor 1, during adsorption are smaller since it takes place during night time. This variations in the inner temperature due to the influence of atmospheric conditions and difference in the driving source temperature of two thermal compressors, leads to significant variations in the density and concentration difference for the refrigerant. Since $\Delta\rho$ is larger and ΔC is smaller for the thermal compressor 2, the uptake efficiency is lower than the thermal compressor 1.

6.6 The optimum heat source temperature for two thermal compressors

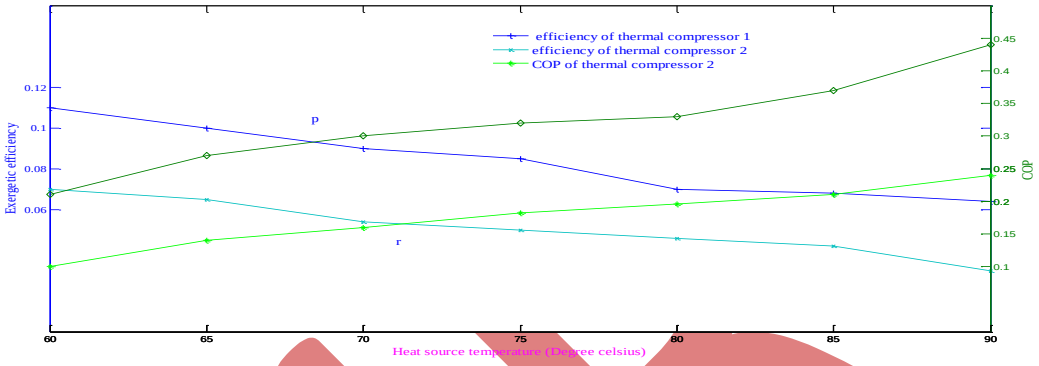

Fig 16 Variation of exergetic efficiency and the coefficient of performance with heat source temperature

For the system, optimum operating point is to be defined. While conducting [21] a study on the effect of heat source temperature on cycle COP and exegy efficiency of the system it is revealed that exergy efficiency decreases and cycle COP increases with the increase in heat source temperature. The optimum heat source temperature is found out by considering the point of intersection of increasing COP curves and decreasing exergy efficiency curves. From the Fig. 16 for this particular system, the optimum heat source temperature for the thermal compressor 1 is found out to be 71.4oC (Point P) where as for the thermal compressor 2 it is 68.20C (point r). This is the point at which cycle COP and exergy efficiency reaches maximum.

6.7 Performance of the network

The performance of the network selected for artificial neural network modeling of solar adsorption refrigeration system is as shown in Table 7.

Table 7

Algorithm LM-9

Parameter	R2	RMS	COV	Mean % deviation
COP day time	0.9959	0.0080	0.0018	1.44
COP night time	0.9935	0.01052	0.0096	1.33
SCP day time	0.9981	0.348	0.00126	0.97
SCP night time	0.9974	0.512	0.00178	3.25
Solar heating COP	0.99024	0.0232	0.1148	2.89
Solar cooling COP	0.9986	0.2803	0.382	1.93

International Journal of Research in Education Methodology
Vol.3 No.1, June 2013, ISSN: 2278-7690

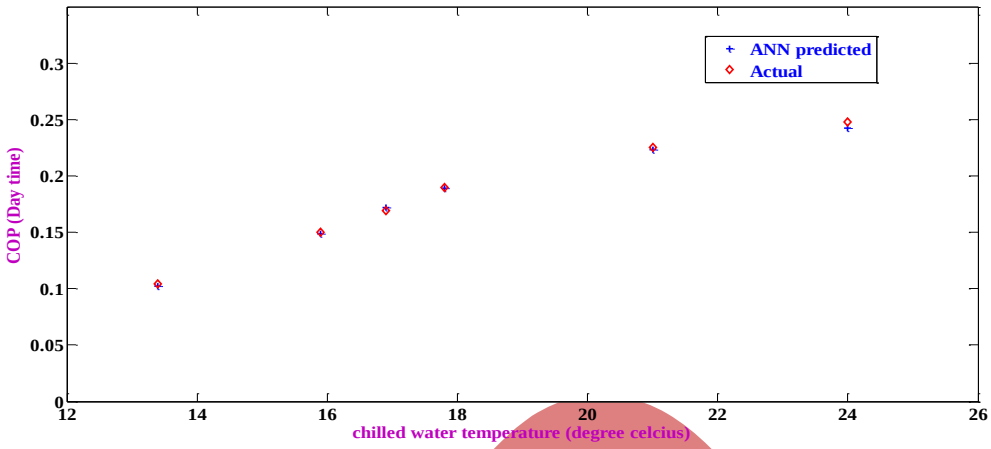

Fig 17. Comparison of actual and ANN predicted values of COP day time

The ANN predicted and experimentally measured COP during day time is given in Fig.17. In this case the ANN predicted COP yields a correlation coefficient of 0.9959 with RMS and COV values 0.0080and 0.0018 respectively.

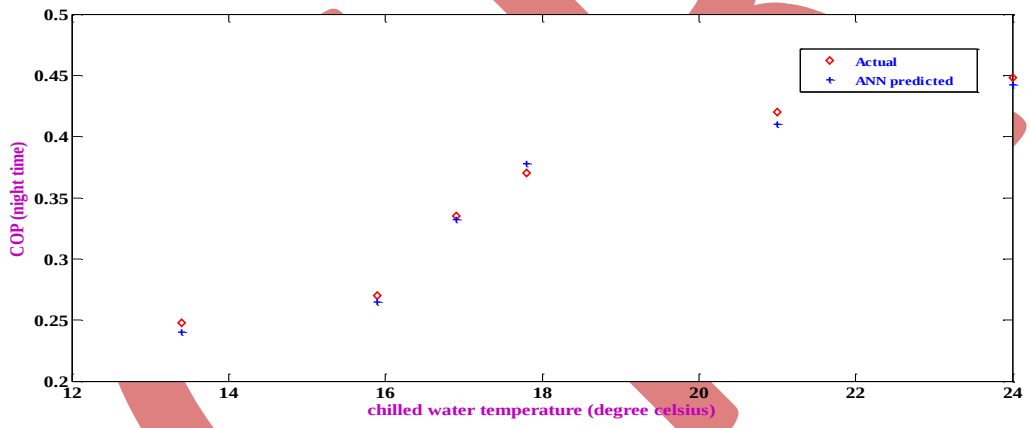

Fig. 18 Comparison of actual and ANN predicted values of COP (night time)

A plot of ANN predicted and experimental COP during night time is depicted in Fig. 18.These predictions yield a correlation coefficient of 0.9935 with RMS and COV values 0.01052 and 0.0096, respectively. The coefficient of performance is an important parameter considered for the rating of SAR system.

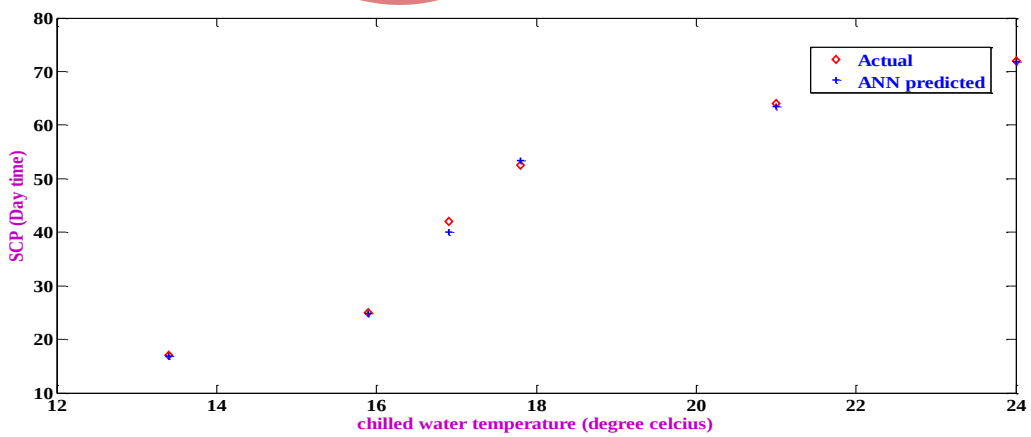

Fig.19 Comparison of ANN predicted and experimentally measured SCP (day time)

International Journal of Research in Education Methodology
Vol.3 No.1, June 2013, ISSN: 2278-7690

The ANN predicted and experimentally obtained SCP values during day time are given in Fig. 19. The ANN predicted COP yields a correlation coefficient of 0.9981 with RMS and COV values 0.348 and 0.00126, respectively.

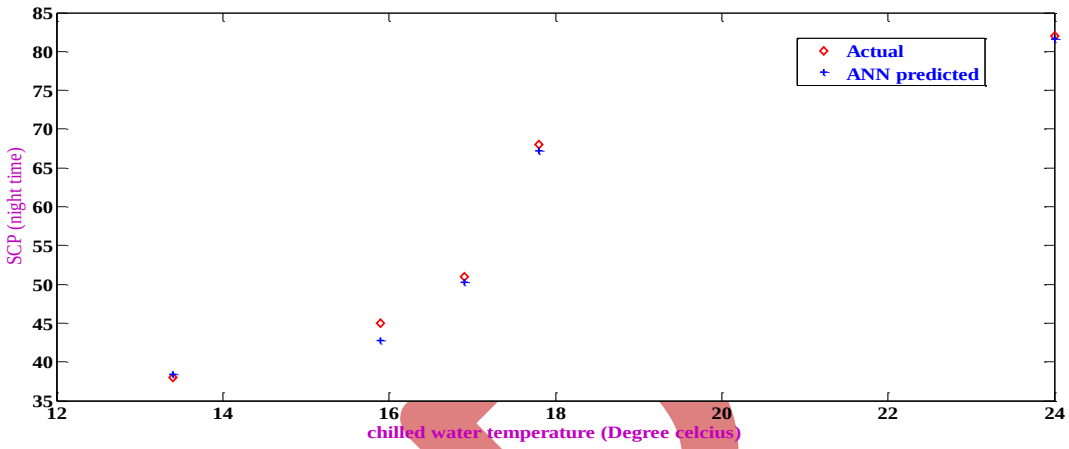

Fig.20 Comparison of actual and ANN predicted values of SCP (night time)

Figure 20 shows experimentally found and ANN predicated values of SCP during night time with the increase in evaporator loads. The ANN predictions yield a correlation coefficient of 0.9974 with RMS and COV values are 0.512 and 0.00178, respectively. Specific cooling power is also a significant parameter that determines the size of the system.

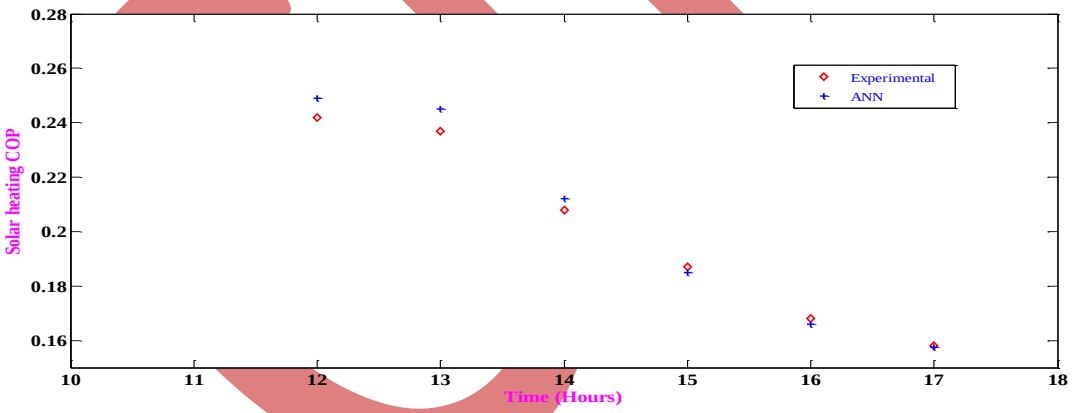

Fig.21 Comparison of actual and ANN predicted values of solar heating COP

The variations of ANN predicted and experimental values of solar heating coefficient of performance with time are shown in Fig. 21. The predictions yield a correlation coefficient of 0.99024 with RMS and COV values 0.0232 and 0.1148, respectively

International Journal of Research in Education Methodology
Vol.3 No.1, June 2013, ISSN: 2278-7690

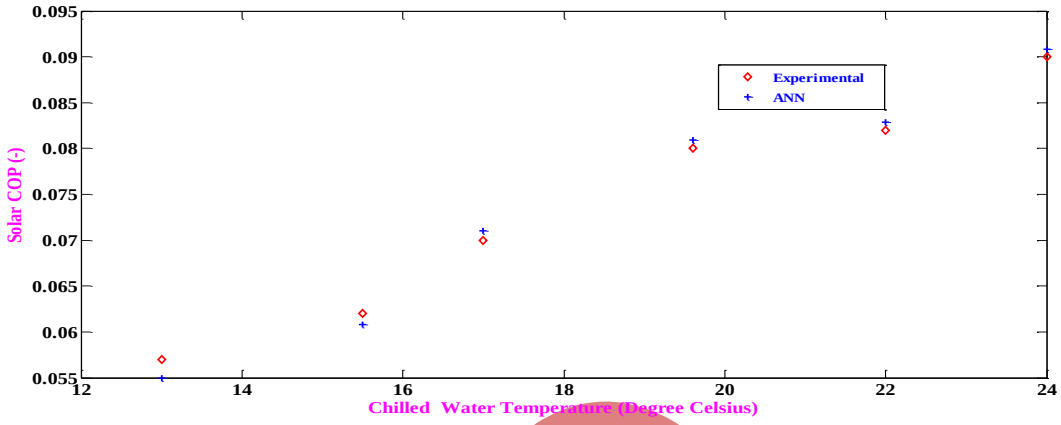

Fig.22 Comparison of actual and ANN predicted values of solar cooling COP

The plot (Fig. 22) of ANN predicted and experimental values of solar cooling COP yields a correlation coefficient of 0.9986 with RMS and COV values 0.2803 and 0.382, respectively. The solar cooling coefficient of performance is significantly considered for determining the performance of a solar collector used in a SAR system. The solar COP is also a prominent parameter that influences the performance of whole system.

Conclusions

This work deals with a two stage solar adsorption refrigeration system which uses solar energy as input. An experimental system was installed and tested for analysing the performance and its thermodynamic cycles. The performance parameters of the system are determined. The main conclusions derivedfrom the present study are given below.

The two stage solar assisted adsorption refrigeration system has been developed for overcoming intermittency of the single bed system. It is found that the system is capable of operating in day time and night time with fairly good performance. The experimental results show that the system has an average refrigerating effect of 60.75 W during day time and 79.87 W during night time.

The mean cycle COP value is obtained as 0.196 during day time and 0.335 during night time. The mean values for specific cooling power for day and night time are 47.83 and 68.2, respectively.

The exergy efficiency of the system is determined for different evaporator loads and the effect of heat source temperature on exergy efficiency and coefficient of performance of the system is studied. The optimum heat source temperature for the thermal compressor 1 is found as 71.4oC and for the thermal compressor 2 it is 68.2oC.

The artificial neural network approach has been applied to the solar hybrid adsorption refrigeration system as an alternative to the classical approaches, which are usually complicated, require an enormous amount of the experimental data and may yield inaccurate results

Using the three different parameters namely temperature, pressure and solar insolation an ANN model based on the back propagation algorithm was proposed. The artificial neural network was used for predicting the performance of the system in terms of coefficient of performance, specific cooling power during day and night time, solar cooling coefficient of performance and solar heating coefficient of performance.

The network model demonstrated good results with correlation coefficients in the range 0.99024-00.9986 and percentage of error 0.97%-3.25%. This study reveals that with the use of neural network, solar adsorption refrigeration systems can be modelled with a high degree of accuracy.

The experimental cycle for the system is obtained for different climatic conditions and it is compared with the theoretical thermodynamic cycle of the system.

REFERENCES

[1] Jung DS, Radermacher R. Performance simulation of single evaporator refrigerator with pure and mixed refrigerants, International Journal of Refrigeration 1991; 14: 223–232.

[2] Chang YS, Kim MS, Ro ST. Performance and heat transfer characteristics of hydrocarbon refrigerants in a heat pump system, International Journal of Refrigeration 2000;23: 232–242.

International Journal of Research in Education Methodology
Vol.3 No.1, June 2013, ISSN: 2278-7690

[3] Van Benthem GHW, Cacciola G, Restuccia G. Regenerative adsorption heat pumps: optimization of the design. Heat Recovery Systems & CHP 1995; 15(6): 31–44.

[4] Critoph RE. Forced convection adsorption cycle with packed bed heat regeneration. ASME international Journal of Refrigeration 1999; 22:38–46.

[5] Pons M. Analysis of the adsorption cycles with thermal regeneration based on the entropic mean temperatures. Applied Thermal Engineering 1997; 17(7): 615–27.

[6] Douss N, Meunier F. Experimental study of cascading adsorption cycles. Chem Engg Sci 1989: 225-35

[7] Cacciola G, Restuccia G. Progress on adsorption heat pumps. Heat Recovery Systems & CHP 1994; 14(4): 409–20

[8] Saha BB, Akisawa A, Kashiwagi T. Solar/waste heat driven two stage adsorption chiller: the prototype. Renewable energy 2001; 23: 93-101.

[9] Critoph RE, Thorpe R. Momentum and heat transfer by forced convection in fixed beds of granular active carbon. Applied Thermal Engineering 1996; 16(5):419–27

[10] Mohanraj M, Jayaraj S, Muraleedharan C. Modeling of a Direct Expansion Solar Assisted Heat Pump Using Artificial Neural Networks, International Journal of Green Energy, 2011; 520 – 532.

[11] Pacheco-Vega A, Sen M, Yang KT, McClain RL. Neural network analysis of fin-tube refrigerating heat exchanger with limited experimental data, International Journal of Heat and Mass Transfer 2001; 44: 763–770.

[12] Kalogirou SA, Bojic M. Artificial neural networks for the prediction of the energy consumption of a passive solar building, Energy 2000; 25: 479–491.

[13] Chouai, S, Laugier, D, Richon. Modeling of thermodynamic properties using neural networks, Application to refrigerants, Fluid Phase Equilibria 2002; 199: 1–10.

[14] nKalogirou SA, Panteliou S, Dentsoras A. Artificial neural networks used for the performance prediction of a thermosiphon solar water heater, Renewable energy 1999;18: 87-99.

[15] Palau A, Velo E, Puigjaner L. Use of neural networks and expert systems to control a gas/solid sorption chilling machine, International Journal of Refrigeration 1999;22: 59–65.

[16] Bechtler H, Browne MW, Bansal PK, Kecman V. New approach to dynamic modeling of vapour-compression liquid chillers: artificial neural networks, Applied Thermal Engineering 2001; 21: 941–953.

[17] Chow TT, Zhang GQ, Lin Z, Song CL. Global optimization of absorption chiller system by genetic algorithm and neural network, Energy and Buildings 2002; 34: 103–109.

[18] Holman JP. Experimental methods for engineers. 7th edition. Tata McGraw-Hill Publishing Company Limited New Delhi

[19] Sumathy K, Zhongfu Li. Experiments with solar powered adsorption ice maker. Renewable Energy 1999; 16: 704 – 707

[20] Akkimaradi BS, Prasad M, Dutta P, Srinivasan K. Effect of packing density and adsorption parameters on the throughput of a thermal compressor, Carbon 2002;40 (15) : 2855-2859.

[21] Baiju V, Muraleedharan C. Performance study of a two stage solar adsorption refrigeration system, International journal of Engineering Science and Technology, 2011; 3: 5754-5764